
STRIDE: Sparse Techniques for Regression in Deep Gaussian Processes

Simon Urbainczyk^{1,2,*} Aretha L. Teckentrup^{2,3} Jonas Latz⁴

¹Heriot-Watt University ²Maxwell Institute for Mathematical Sciences

³University of Edinburgh ⁴University of Manchester

Abstract

Gaussian processes (GPs) have gained popularity as flexible machine learning models for regression and function approximation with an in-built method for uncertainty quantification. However, GPs suffer when the amount of training data is large or when the underlying function contains multi-scale features that are difficult to represent by a stationary kernel. To address the former, training of GPs with large-scale data is often performed through inducing point approximations (also known as sparse GP regression (GPR)), where the size of the covariance matrices in GPR is reduced considerably through a greedy search on the data set. To aid the latter, deep GPs have gained traction as hierarchical models that resolve multi-scale features by combining multiple GPs. Posterior inference in deep GPs requires a sampling or, more usual, a variational approximation. Variational approximations lead to large-scale stochastic, non-convex optimisation problems and the resulting approximation tends to represent uncertainty incorrectly. In this work, we combine variational learning with MCMC to develop a particle-based expectation-maximisation method to simultaneously find inducing points within the large-scale data (variationally) and accurately train the GPs (sampling-based). The result is a highly efficient and accurate methodology for deep GP training on large-scale data. We test our method on standard benchmark problems.

1 Introduction

Gaussian process regression is a popular Bayesian methodology in supervised learning, non-parametric statistics, and function approximation, with a variety of favourable features such as tractable inference and uncertainty quantification. When GPs are not sufficiently flexible, we can construct deep GPs by, e.g., sequentially composing a number of otherwise independent GPs. Deep GPR retains many features of GPR, but importantly makes posterior inference much more computationally challenging. Sampling-based techniques for deep GPR require repeated GPR steps – infeasible if the number of observed data sets is large. In the present work, we propose STRIDE a method that combines Markov chain Monte Carlo (MCMC) with sparse GPR for an accurate and computationally efficient deep GPR. Indeed, we

- (i) propose a sparse-Gaussian-process-marginalised MCMC sampler for deep Gaussian process regression,
- (ii) propose a heuristic greedy algorithm to find inducing points by optimising a deep variational lower bound,
- (iii) construct STRIDE by combining (i), (ii) in a Monte Carlo Expectation-Maximisation methodology,

*Corresponding author: su2004@hw.ac.uk.

- (iv) discuss approximate sampling techniques on lower deep Gaussian process layers to reduce the overall complexity to linear in the size of the training dataset,
- (v) verify our methodology in usual benchmark problems and in a large-scale Fashion-MNIST problem, where it beats comparable sparse Gaussian processes.

After a literature review, we collect the technical background in conventional, deep, and sparse GPR in Section 2, before we derive STRIDE in Section 3, summarise our experiments and their results in Section 4, and conclude in Section 5.

Literature review. Sparse GPR is a popular tool for solving regression problems involving large numbers of data points, see e.g. the works [7, 35, 38, 41] as well as the unifying perspectives [3, 30]. In STRIDE, we focus on the objective function described in [38] to select optimal inducing points.

In the context of deep GPR, the posterior needs to be approximated with samples, e.g. through MCMC [14, 23, 24, 34], or a variational approximation [8–10, 19]. Variational approximations are popular due to their scalability, but challenges remain as they require non-convex large-scale optimisation, tend to misrepresent uncertainty, and are not yet fully understood theoretically [2]. In this work, we therefore focus on provably convergent MCMC methods for reliable uncertainty quantification. Sparse GPR techniques based on [38] have successfully been employed in variational approximations of deep GPs [10, 11], as well as the related setting of hierarchical GPs with hyper-parameters [32].

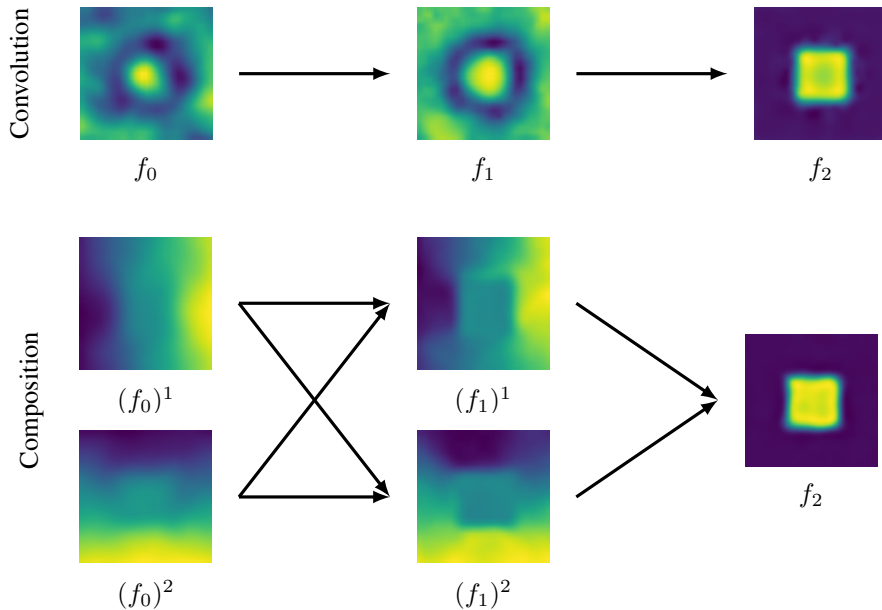


Figure 1: Illustration of 3-layer deep Gaussian processes with convolution (top) and composition (bottom) architectures. The input dimension is $d = 2$. The deep GPs have been conditioned with respect to data from a simple piecewise-constant target.

Deep GPs can be constructed in a variety of ways, typically based on a hierarchical approach to non-stationary GP modelling [14, 33]. When combining the individual GP layers in said hierarchical fashion, the most prominent example is the composition architecture as described in the seminal papers [10, 15]. The convolution architecture, on the other hand, uses the individual GP layers to define a non-stationary correlation length for the next layer [14, 31]. We illustrate both architectures in Figure 1. A synthesis of composition and convolution architectures was recently proposed in [12].

STRIDE is based on the expectation-maximisation (EM) algorithm [13, 36]. We also refer to [25] for variants of EM, including Monte Carlo EM [39] which is used in this work. While we combine preconditioned Crank–Nicolson (pCN) MCMC [6] for the expectation step and a greedy method for the maximisation step, previous works have combined Langevin sampling and gradient flows [20, 22] in a similar context.

2 Gaussian process regression and extensions

In the following we consider the following supervised learning problem: we are given data pairs $(x_i, y_i)_{i=1}^n \in (\mathbb{R}^d \times \mathbb{R})^n$ through $f^\dagger(x_i) + \varepsilon_i = y_i$, where f^\dagger is an unknown function and $\varepsilon_1, \dots, \varepsilon_n \sim N(0, \gamma^2)$ i.i.d. is observational noise. Our goal is to recover the function f^\dagger from the observational data. GPR is a natural Bayesian strategy to approach problems of this form. Given a prior $\text{GP}(0, k(\cdot, \cdot))$, we obtain the posterior $\text{GP}(\mu^y(\cdot), k^y(\cdot, \cdot))$, with

$$\begin{aligned} \mu^y(\cdot) &= k(\cdot, \mathbf{x}_n) (k(\mathbf{x}_n, \mathbf{x}_n) + \gamma^2 \text{Id})^{-1} \mathbf{y}_n, \\ k^y(\cdot, \cdot) &= k(\cdot, \cdot) - k(\cdot, \mathbf{x}_n) (k(\mathbf{x}_n, \mathbf{x}_n) + \gamma^2 \text{Id}_n)^{-1} k(\mathbf{x}_n, \cdot). \end{aligned} \quad (1)$$

Here, the bold letters refer to the full data sets $\mathbf{x}_n := (x_i)_{i=1}^n$ and $\mathbf{y}_n := (y_i)_{i=1}^n$. When kernels are applied to these sets, we obtain kernel matrices/vectors.

In the following, we discuss two extensions of GPR: deep GPR in cases where GPs are not sufficiently flexible (Subsections 2.1, 2.2) and sparse GPR as a computationally efficient approximation of GPR (Subsection 2.3).

2.1 Deep Gaussian processes

A sequence of random functions $(f_\ell)_{0 \leq \ell \leq L}$ is called a *deep Gaussian process* with $L + 1$ layers if f_0 is a Gaussian process, and if f_ℓ is conditionally Gaussian for $\ell \geq 1$, i.e.

$$\pi_{f_\ell | f_{\ell-1} = u_{\ell-1}} = \text{GP}(0, k_\ell(\cdot, \cdot | u_{\ell-1})),$$

for any realisation $u_{\ell-1}$ of $f_{\ell-1}$.

The properties of a deep GP strongly depend on the choice of the conditional covariance kernel k_ℓ , which determines its architecture. We consider two approaches here, namely, the convolution architecture described in [14, 27], as well as the composition/warping architecture [10, 14, 34].

Convolution. Covariance kernels are often constructed in the following way: we define an isotropic correlation function $\rho : \mathbb{R} \rightarrow \mathbb{R}$ and then obtain a covariance kernel through $k(x, x') = \sigma^2 \rho(\|x - x'\| / \lambda)$ for some marginal variance $\sigma^2 > 0$ and correlation length $\lambda > 0$. The correlation length determines the strength of long-range correlation in a GP and, thus, the oscillatory behaviour of its samples. In the convolution architecture, we now use a spatially-dependent value for λ that is given through the realisation $u_{\ell-1}$ of the next-lower deep GP layer $f_{\ell-1}$. A spatially variable correlation length allows us to describe multi-scale behaviour in a function, e.g., in images. We usually set $\lambda(x) := h(u_{\ell-1}(x))$, where $h : \mathbb{R} \rightarrow \mathbb{R}_+$ is some non-negative transformation of the hidden layer values $u_{\ell-1}$. More precisely, in a multi-layer setting, we give the covariance function k_ℓ as,

$$k_\ell^{\text{conv}}(x, x' | u_{\ell-1}) = \sigma^2 \phi(x, x') \rho\left(\frac{2 \|x - x'\|}{h(u_{\ell-1}(x)) + h(u_{\ell-1}(x'))}\right),$$

where

$$\phi(x, x') = \frac{2^{d/2} h(u_{\ell-1}(x))^{d/4} h(u_{\ell-1}(x'))^{d/4}}{(h(u_{\ell-1}(x)) + h(u_{\ell-1}(x')))^{d/2}}, \quad h(z) = \min(\max(z, u^{\min}), u^{\max})^2.$$

In the above, the pre-factor $\phi(x, x')$ ensures that the resulting covariance function remains positive semi-definite. The scalar transformation $h : \mathbb{R} \rightarrow \mathbb{R}^+$ given here is an example that worked well in our experiments, with u^{\min}, u^{\max} as tunable parameters. Other functions that result in positive correlation length values would also be valid. Note that the correlation length can in principle be chosen to be matrix-valued, but we restrict ourselves to scalars in this work, see [14, 27].

Composition. The composition architecture tries to identify a transformation of the input space that best enables the top layer to model the data. That is, the layer realisations are now given by functions u_ℓ that map \mathbb{R}^{d_ℓ} into $\mathbb{R}^{d_{\ell+1}}$, where $d_0 = d$ and $d_{L+1} = 1$. Starting with a stationary kernel k , the generally non-stationary kernel of f_ℓ is then given by,

$$k_\ell^{\text{comp}}(x, x' | u_{\ell-1}) = k(u_{\ell-1}(x), u_{\ell-1}(x')).$$

In this case, some of the layers may be multi-output GPs.

2.2 Deep Gaussian process regression

The posterior in deep GPR is commonly approximated with samples, e.g. through MCMC [14, 23, 24, 34]. Here we especially note a helpful trick in MCMC for deep GPR: marginalising the outer layer: Bayes' theorem implies that

$$\pi_{f_L, \dots, f_0 | \mathbf{y}_n} = \frac{\pi_{\mathbf{y}_n | f_L} \pi_{f_L, \dots, f_0}}{\pi_{\mathbf{y}_n}} = \underbrace{\frac{\pi_{\mathbf{y}_n | f_L} \pi_{f_L | f_{L-1:0}}}{\pi_{\mathbf{y}_n | f_{L-1:0}}}}_{(*)} \underbrace{\frac{\pi_{\mathbf{y}_n | f_{L-1:0}} \pi_{f_{L-1:0}}}{\pi_{\mathbf{y}_n}}}_{(**)},$$

where $f_{L-1:0} := f_{L-1}, \dots, f_0$ and

(*) is the conditional outer layer posterior $\pi_{f_L | \mathbf{y}_n, f_{L-1:0}}$ and given through (1),

(**) is the inner layers posterior $\pi_{f_{L-1:0} | \mathbf{y}_n}$ that can be sampled with MCMC.

Hence, the MCMC method needs to only approximate the posterior distributions on the lower layers $f_{L-1:0}$, but not the outer layer f_L .

2.3 Sparse Gaussian process regression

In GPR, the inversion of the kernel matrix becomes a computational challenge for large numbers of observations n . The idea of sparse GPR is to reduce the size of this matrix by representing the observed data through a number of ‘‘virtual’’ observations, or inducing variables. We denote the number of inducing variables by m , and generally choose $m \ll n$. We then construct an approximate posterior $\pi_{f | \mathbf{y}_n}^{\mathcal{M}}$ that only requires us to work with $n \times m$ and smaller matrices.

Suppose we have chosen a subset of the indices of the observational data points, $\mathcal{M} \subset [n]$ with $|\mathcal{M}| = m$, to represent our inducing points. Here, $[n]$ denotes the set $[n] = \{i \in \mathbb{N} \mid i \leq n\}$. Let $p : [m] \rightarrow [n]$ denote a mapping that assigns each observation selected as an inducing point its corresponding index in the data $(x_i, y_i)_{i=1}^n$. Using this mapping, define the matrices $K_{mm} \in \mathbb{R}^{m \times m}$ and $K_{mn} \in \mathbb{R}^{m \times n}$, as well as the vector of covariances $K_m(x) \in \mathbb{R}^m$, element-wise as

$$(K_{mm})_{j,j'} = k(x_{p(j)}, x_{p(j')}), \quad (K_{mn})_{j,i} = k(x_{p(j)}, x_i), \quad (K_m(x))_j = k(x_{p(j)}, x),$$

where $i \in [n]$, $j, j' \in [m]$, $x \in \mathbb{R}^d$.

In selecting the inducing points from the observations, we follow [38]. We choose inducing points represented by indices \mathcal{M} that minimize the KL divergence between an approximate posterior $\pi_{f | \mathbf{y}_n}^{\mathcal{M}}$ and the posterior $\text{GP}(\mu^y(\cdot), k^y(\cdot, \cdot))$. As is shown in [37, 38], this KL divergence can be minimised by maximising the variational lower bound,

$$F_V(\mathcal{M}) \propto -\frac{1}{2} \mathbf{y}_n^T (K_{mn}^T K_{mm}^{-1} K_{mn} + \gamma^2 \text{Id}_n)^{-1} \mathbf{y}_n - \frac{1}{2} \log \det(K_{mn}^T K_{mm}^{-1} K_{mn} + \gamma^2 \text{Id}_n) - \frac{1}{2\gamma^2} \text{trace}(K_{rr} - K_{mr}^T K_{mm}^{-1} K_{mr}). \quad (2)$$

In the above, the subscript r used for matrices K_{rr} and K_{mr} denotes the observational data indices that are not included as inducing points. That is,

$$K_{rr} = (k(x_i, x_j))_{i \in [n] \setminus \mathcal{M}, j \in [n] \setminus \mathcal{M}}, \quad K_{mr} = (k(x_i, x_j))_{i \in \mathcal{M}, j \in [n] \setminus \mathcal{M}}.$$

The approximate posterior $\pi_{f | \mathbf{y}_n}^{\mathcal{M}} = \text{GP}(\mu_{\mathcal{M}}, k_{\mathcal{M}}(\cdot, \cdot))$ obtained with sparse GPR is given then by

$$\mu_{\mathcal{M}}(x) = \gamma^{-2} K_m(x)^T (K_{mm} + \gamma^{-2} K_{mn} K_{mn}^T)^{-1} K_{mn} \mathbf{y}_n, \\ k_{\mathcal{M}}(x, x') = k(x, x') - K_m(x)^T K_{mm}^{-1} K_m(x') + K_m(x)^T (K_{mm} + \gamma^{-2} K_{mn} K_{mn}^T)^{-1} K_m(x').$$

Note that these formulas only use the inverse of $m \times m$ matrices, as opposed to $n \times n$ for standard GPR. Likewise, the memory needed to store the covariance matrices is reduced to $\mathcal{O}(mn)$.

3 Inducing points for deep Gaussian process regression

When using the marginalisation strategy in Subsection 2.2, we need to repeatedly evaluate $\pi_{\mathbf{y}_n|f_{L-1}, \dots, f_0}$. Each of the latter evaluations requires a GPR step, which is prohibitively expensive if n is large. In the following, we introduce an iterative procedure that allows us find a set of inducing points \mathcal{M} that help us to construct approximate distributions $\pi_{f_L|\mathbf{y}_n, f_{L-1:0}}^{\mathcal{M}}$, $\pi_{f_{L-1:0}|\mathbf{y}_n}^{\mathcal{M}}$, and $\pi_{\mathbf{y}_n|f_{L-1:0}}^{\mathcal{M}}$ through sparse GPR and, thus, enable deep GPR under large-scale data.

In particular, our goal is in the following to find a set of inducing points \mathcal{M} that maximises

$$F(\mathcal{M}) = \int F_V(\mathcal{M}; u_{L-1:0}) d\pi_{f_{L-1:0}|\mathbf{y}_n}^{\mathcal{M}}(u_{L-1:0}),$$

where $F_V(\mathcal{M}; u_{L-1:0})$ is given as in (2), but with the covariance kernel $k := k_L$ depending on lower layers $u_{L-1:0}$. To minimise F , we propose a Monte Carlo Expectation-Maximisation (MCEM) method [39]. In MCEM methods, we maximise objectives such as F by alternately approximating the distribution $\pi_{f_{L-1:0}|\mathbf{y}_n}^{\mathcal{M}}$ given some \mathcal{M} (expectation step) and by using this approximation to maximise an empirical approximation of $F(\mathcal{M})$ and, thus, obtain an improved index set (maximisation step).

Let $P_{\mathcal{M}}$ be an MCMC kernel, i.e., a Markov kernel that is stationary with respect to $\pi_{f_{L-1:0}|\mathbf{y}_n}^{\mathcal{M}}$ and ergodic. We then construct a sequence of particles and inducing point sets $(f_{L-1:0}^{(s,t)}, \dots, f_{L-1:0}^{(S,t)}, \mathcal{M}_t)_{t \geq 0}$, where S denotes the number of particles and t denotes time. Particles and sets are given through the following two-step iteration.

(E) Given inducing points \mathcal{M}_t , sample $f_{L-1:0}^{(s,t+1)} \sim P_{\mathcal{M}_t}(\cdot | f_{L-1:0}^{(s,t)})$ for $s = 1, \dots, S$.

(M) Given particles $(f_{L-1:0}^{(s,t+1)})_{s=1}^S$, update the inducing points through

$$\mathcal{M}_{t+1} \in \operatorname{argmax}_{\mathcal{M}} \frac{1}{S} \sum_{s=1}^S F_V(\mathcal{M}; f_{L-1:0}^{(s,t+1)}).$$

We refer to the above method as *STRIDE*. Here, **(E)** corresponds to the expectation step, and the **(M)** to the maximisation step in this MCEM algorithm, respectively. We terminate the method at a large $T \in \mathbb{N}$, the final model is then given by

$$\frac{1}{S} \sum_{s=1}^S \operatorname{GP}\left(\mu_{\mathcal{M}_T}(\cdot | f_{L-1:0}^{(s,T)}), k_{\mathcal{M}_T}(\cdot, \cdot | f_{L-1:0}^{(s,T)})\right).$$

Both expectation and maximisation steps will be described in more detail in the following two subsections. Following this, we discuss computationally efficient strategies on the lower layers.

3.1 Monte Carlo expectation step

We first describe the procedure employed to obtain samples $(f_{L-1:0}^{(s,t+1)})_{s=1}^S$, as required in the expectation step **(E)** of *STRIDE*. Given some inducing points \mathcal{M}_t , we want sample the hidden parameter from the density $\pi_{f_{L-1:0}|\mathbf{y}_n}^{\mathcal{M}}$. This density is given through Bayes' Theorem

$$\pi_{f_{L-1:0}|\mathbf{y}_n}^{\mathcal{M}} \propto \pi_{\mathbf{y}_n|f_{L-1:0}}^{\mathcal{M}} \pi_{f_{L-1:0}},$$

see also (**). Combining the covariance structure defined by $f_{L-1:0}$ and \mathcal{M}_t with the observational noise covariance, we can express the likelihood term as,

$$\pi_{\mathbf{y}_n|f_{L-1:0}}^{\mathcal{M}} \propto \frac{1}{\sqrt{\det Q_{nn}(f_{L-1:0})}} \exp\left(-\frac{1}{2} \|\mathbf{y}_n\|_{Q_{nn}(f_{L-1:0})}^2\right),$$

$$Q_{nn}(f_{L-1:0}) = K_{mn}(f_{L-1:0})^T K_{mm}(f_{L-1:0})^{-1} K_{mn}(f_{L-1:0}) + \gamma^2 \operatorname{Id}_n.$$

The logarithmic likelihood (omitting constants) is identical to the first two terms in our definition of F_V in (2). In order to compute samples of this density, we employ a Monte Carlo Markov chain

(MCMC) algorithm. In particular, we whiten the prior $\pi_{f_{L-1:0}}$ [28, 43] and then apply the pCN proposal [6].

We note that the determinant of $Q_{nn}(f_{L-1:0})$ can be computed in $\mathcal{O}(m^3)$ using the Weinstein–Aronszajn identity. We usually employ multiple subsequent MCMC steps in a single expectation step to ensure that the particles approximate $\pi_{f_{L-1:0}|\mathbf{y}_n}^{\mathcal{M}}$ well.

3.2 Maximisation step

During the maximisation step (**M**) of STRIDE, we aim at finding a set of inducing points \mathcal{M}_{t+1} that maximises the expected value of $F_V(\mathcal{M}; f_{L-1:0})$, which we approximate by

$$\frac{1}{S} \sum_{s=1}^S F_V(\mathcal{M}; \theta_{t+1}^{(s)}) =: F_t(\mathcal{M}).$$

Finding the global minimiser of F_t likely requires an enumeration of $\{\mathcal{M} \subseteq [n] : |\mathcal{M}| = m\}$ which is infeasible. Instead, we follow a heuristic greedy strategy. We select the initial set of inducing points \mathcal{M}_0 in the algorithm using a strategy motivated by [38]: starting from an empty set, we add the observation that leads to the biggest increase of the objective. In practice, one chooses these observations from sets of candidate points \mathcal{J} with cardinality $|\mathcal{J}| \ll n$ that are sampled randomly at each step to preserve computational efficiency. Elements are added in this greedy fashion until the maximum cardinality m is reached.

When updating an existing set \mathcal{M}_t to obtain \mathcal{M}_{t+1} in STRIDE, we proceed as follows. We loop over every element in \mathcal{M}_t and measure its contribution to the overall objective value by excluding it from \mathcal{M}_t and evaluating F_t . In this way, we determine the element that, through exclusion, *decreases F_t the least*, and exclude it from \mathcal{M}_t . We then loop over all observations in a set of candidates $\mathcal{J} \subset [n] \setminus \mathcal{M}_t$ to determine the element that, through adding, *increases F_t the most*. We then include this element in our set of inducing points. This procedure can be repeated for a number of iterations. We choose the resulting set of inducing points as our updated set, \mathcal{M}_{t+1} . As mentioned, the set \mathcal{J} is generally chosen to be of fixed cardinality $|\mathcal{J}| \ll n$ to control the cost of the update. As a result, the number of evaluations of F_t needed for the update step is $R(m + |\mathcal{J}|)$, where R is the number of update step repetitions.

3.3 Linear complexity on lower layers

The main advantage of using sparse GPR methods such as [38] is that they can be computed with an $\mathcal{O}(n)$ cost, as opposed to $\mathcal{O}(n^3)$ for standard GPR. We aim at preserving this property in STRIDE. However, in order to be able to choose \mathcal{J} as a subset of the observations, we need to evaluate the hidden layers of the deep GP at every observed location. This leads to having to construct covariance matrices of size $n \times n$, and sampling the hidden layers to obtain the covariance of the top layer then results in a computational cost of $\mathcal{O}(n^3)$, which is the complexity of the required Cholesky decomposition. We now propose two approaches for efficient computation on the lower layers.

Adaptive cross approximation. We can sample the hidden layers approximately using an approach that is cheaper than $\mathcal{O}(n^3)$. In our experiments, we use an adaptive cross-approximation (ACA) algorithm [17, 18, 21], which approximates the Cholesky factor of the covariance matrix. More specifically, ACA determines a set of indices that identify the columns of the covariance matrix that can be used for an accurate low-rank approximation of the same covariance matrix. One can either select this set of indices once at the start of our EM algorithm and leave it fixed throughout, or, after each maximisation step (**M**), recompute the set of indices to reflect that the covariance matrix we aim to approximate has changed. In our experiments using ACA, we employ this latter approach. However, note that, since we are sampling whitened variables in the expectation step (**E**), this means that we also need to update these sampled variables to ensure they represent the same hidden parameters $f_{L-1:0}$ after updating our approximation of the covariance.

Fully sparse. We can sample the hidden layers at the current inducing points only. In this case, sampling the hidden layers becomes very cheap. The covariance at the top layer is then based on an interpolation of the next-lower layer to all observation locations. We perform this interpolation using standard GPR. The covariance kernel used here constitutes another set of tuning parameters.

In practice, we simply use a stationary GP with the same marginal variance, correlation length and observation noise variance that the deep GP itself is initialised with. Using this “fully sparse” approach of sampling only at the inducing point locations also means that we need to update our hidden parameters every time we change the inducing points \mathcal{M}_t . That is, once the inducing points change, we now need evaluations of the hidden layers at these new locations. Once more, we obtain these through interpolation using GPR.

4 Numerical experiments

We now put our algorithm to the test in a number of real-life regression problems. In a first step, we consider the performance in three small-scale regression problems using datasets from the UCI Machine Learning Repository.² Since the deep GP can be specified in a multitude of ways, we use these examples to explore a range of possible setups. Mainly, we aim to investigate the effect of the deep GP construction type, as well as number of hidden layers. In a second experiment, we test the performance of our approach on a variation of the FashionMNIST dataset [42]. Namely, we consider features extracted using an auto-encoder, as presented in [5].³ This dataset is much larger (70,000 points with 30 dimensions) than the UCI datasets considered, and as such poses a significant computational challenge. Most importantly, standard GPR becomes infeasible on such large datasets, so that we have to resort to sparse GPR methods. All experiments were performed on an AMD EPYC 7513 32-core processor; we allocated 16 GB of RAM.

4.1 Standard UCI datasets

For our first experiment, we consider the energy efficiency, the concrete compressive strength, and the Boston housing datasets from the UCI Machine Learning Repository. These are relatively small, with numbers of data points ranging from 506 to 992. As a result, we can evaluate standard GPR on these datasets, and use the results for comparison. As we are using their strategy for selecting inducing points, we also compare with the sparse GPR approach from [38]. Furthermore, the datasets are small enough to run deep GPR without making use of inducing points. We refer to this as “standard” deep GPR. Both standard GPR and standard deep GPR would quickly become infeasible for larger datasets, since their computational cost grows cubically.

The goal of our experiment is to get an overview of the effect of choosing different architectures and approximation methods of the hidden layers. Our setup is as follows. The kernel k is chosen as the Gaussian kernel, also known as the squared exponential or RBF kernel. The marginal variance, correlation length and observation noise variance are estimated through likelihood maximisation for the standard GP, and through maximising F_V as given in (2) for the sparse GP approach. The optimal hyper-parameters found in sparse GPR are then used to set up our deep GP model. That is, we use the same noise variance, and set the marginal variance of the top layer to the marginal variance obtained through optimisation. The marginal variances of the hidden layers are set to 1. The hidden layers $f_{L-1;0}^{(s,0)}$ are initialised so that the resulting covariance of the top layer is stationary with the correlation length found through hyper-parameter optimisation for each of the particles, $s = 1, \dots, S$.

For each model relying on inducing points, we select m as 50. We run STRIDE for 10 EM iterations, each expectation step (E) consisting of 400 MCMC steps, and each maximisation step (M) consisting of 5 inducing point update steps. As a maximum size of the candidate set in the update steps, $|\mathcal{J}|$, we choose 500. We simulate $S = 50$ different particles each time.

We use ten-fold cross-validation on each of the datasets to evaluate the errors of our individual GP and deep GP setups. Namely, we compute the standardised mean square error (SMSE; smaller values are better) as defined in [40]. The results are shown in Figure 2. In the left two plots, we obtain the SMSE for the energy efficiency dataset, using two and three layers in the deep GP models, respectively. In the third plot from the left, we show SMSE values for the concrete compressive strength dataset and in the plot on the right we consider the Boston housing dataset. For these last two plots, we use two layers in the deep GP models. We give the mean of the error values over the ten training/test data splits, as well as error bars of twice the standard deviation. The deep GP architectures are given in

²These datasets can be found at <https://archive.ics.uci.edu/>.

³The dataset used is available at https://github.com/jwcalder/GraphLearning/blob/master/kNNDData/FashionMNIST_vae.npz.

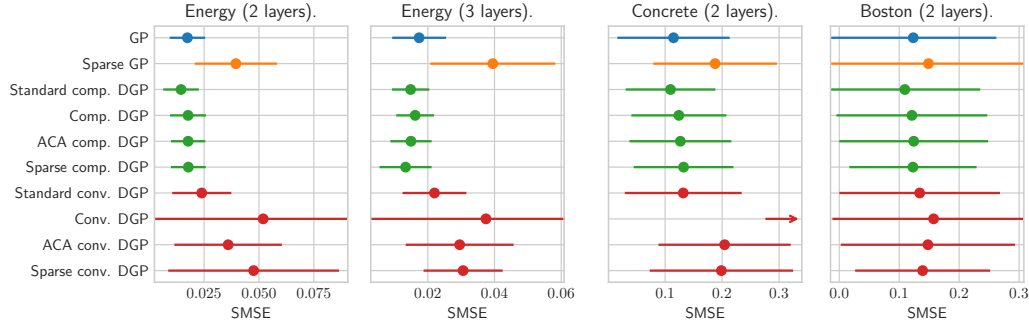


Figure 2: Overview of obtained SMSE values in ten-fold cross-validation for three UCI datasets.

abbreviated form (“comp.” and “conv.”). The use of our two approaches to approximating hidden layers is marked by either “ACA” or “sparse”.

We observe that for all three datasets, using full GPR gives better results than sparse GPR, which is expected. Using a deep GP, we obtain similar, or sometimes better performance than the standard GP. Generally, the standard deep GP performs best for each architecture, giving an indication of how much using a non-stationary model could improve the error on the dataset in question. The setups using an inducing points approximation on the top layer then perform similarly. However, we note that there is a large variance in the reconstruction errors when using the convolution architecture when sampling the full hidden layers. In particular, this setup fails to satisfyingly perform regression on the concrete dataset, leading to errors larger than 1 (as indicated by an arrow here). Approximating the hidden layers (using ACA or the fully sparse approach) appears to have a regularising effect when using the convolution architecture, as the SMSE values for these approaches are much closer to the standard deep GP values.

Generally speaking, the standard deviations shown around the mean errors are especially large in the plot concerning the Boston housing dataset, as the regression results varied significantly between different splits of the data. However, we can still observe that the deep GP models appear to represent the data more accurately than the stationary GP models. When comparing the two different deep GP constructions, the composition architecture results in a better prediction error for each of the datasets. A reason could be that the convolution architecture makes use of GP layers with a one-dimensional output only, so that it is less flexible when storing information on the hidden layers compared to the composition architecture. We further note that using three instead of two layers improves the regression result for the energy efficiency dataset. The reduction in error can be substantial and can be observed for each of the deep GP setups.

We briefly analyse the compute times for the composition architecture with two layers on the energy efficiency dataset. For a single run, using the standard deep GP took 3,116 s of (offline) training, as well as 12.74 s for the prediction on the test data, in what can be considered the online cost. When using STRIDE, the training time was reduced to 1,069 s, and the prediction time went down to 0.095 s. Using ACA and the fully sparse approach resulted in similar training times for this relatively small dataset (1,323 s and 1,181 s, respectively). The prediction time for ACA was 0.093 s, and 0.057 s for the fully sparse approach.

4.2 Large dataset (Fashion MNIST)

We now turn towards performing regression on a more challenging dataset. Fashion MNIST is a popular benchmark for machine learning methods, containing 70,000 greyscale images, each associated with a class label represented by an integer number [42]. As the images are of dimension 28×28 , the computational burden of using a deep GP with the composition architecture would make regression infeasible. However, the dimension of the data points can be reduced by techniques such as variational auto-encoders (VAEs) [5]. In our case, we use a variant of the dataset where the data points have already been transformed by such a VAE.

We want to explore the effect of the number of inducing points, m . To this end, we run sparse GPR [38], as well as STRIDE using the composition architecture and ACA with rank 50 to approximate

Table 1: SMSE values obtained for different values of m .

m	50	75	100	125
Sparse GP	0.2358	0.2360	0.2246	0.2169
STRIDE	0.2347	0.2219	0.2116	0.2063

the hidden layer. In STRIDE, we now use $S = 10$ Markov chains as well as $R = 3$ individual updates of the inducing points in each maximisation step (**M**) only. The size of the candidate set is chosen as $|\mathcal{J}| = 1000$. Otherwise, the setup remains the same as in the previous experiment in Section 4.1. As the training data we use a random selection of 90% of the dataset, leaving the remaining 10% as the test set. We repeat this experiments for m ranging from 50 to 125. The obtained SMSE values are presented in Table 1. Notably, the reported errors decrease as expected as we increase m . Even for small numbers of m , we obtain a more accurate regression result when using the deep GP model. However, even for sparse GPR, the errors do not stagnate as we increase m , indicating that this dataset requires large numbers of inducing points for an accurate representation.

5 Conclusion

In the above, we have introduced STRIDE, a scalable technique for performing fully Bayesian deep GPR. This method combines the computational savings of sparse GPR with the flexibility of deep GP models and the accurate uncertainty quantification provided by MCMC. We furthermore describe two approaches to approximating the covariance matrices of the hidden layers of the deep GP. In conjunction with STRIDE, this results in a method whose computational cost scales linearly with respect to the number of observations. In experiments on standard datasets, we showed that STRIDE indeed reaches regression accuracies similar to, and sometimes better than, the usually intractable standard GPR, and beats sparse GPR. Thus, STRIDE is a computationally efficient methodology for Bayesian machine learning.

Important future research directions are generalisations of STRIDE to non-Gaussian likelihoods, the SASPA framework might be a useful point to start [29]. Moreover, we have not analysed STRIDE in this work, techniques from [1, 4, 16, 26] might support a convergence analysis.

Limitations. STRIDE makes deep GPR more scalable, but does not remove every limitation deep or standard GPR has. Especially the use of STRIDE with high input dimension d without separate feature extraction, for instance, should still be very challenging. STRIDE profits from sparse GPR, but the more flexible deep GP models still require more computational resources.

Acknowledgments and Disclosure of Funding

SU, ALT, and JL acknowledge the use of the HWU high-performance computing facility (DMOG) and associated support services in the completion of this work. ALT was partially supported by EPSRC grants EP/X01259X/1 and EP/Y028783/1.

References

- [1] Kweku Abraham and Neil Deo. Deep Gaussian process priors for Bayesian inference in nonlinear inverse problems. *arXiv preprint arXiv:2312.14294*, 2023.
- [2] David M. Blei, Alp Kucukelbir, and Jon D. McAuliffe and. Variational inference: A review for statisticians. *Journal of the American Statistical Association*, 112(518):859–877, 2017.
- [3] Thang D. Bui, Josiah Yan, and Richard E. Turner. A unifying framework for Gaussian process pseudo-point approximations using power expectation propagation. *Journal of Machine Learning Research*, 18(104):1–72, 2017.

- [4] David R. Burt, Carl Edward Rasmussen, and Mark van der Wilk. Convergence of sparse variational inference in Gaussian processes regression. *Journal of Machine Learning Research*, 21(131):1–63, 2020.
- [5] Jeff Calder, Brendan Cook, Matthew Thorpe, and Dejan Slepcev. Poisson learning: Graph based semi-supervised learning at very low label rates. In *International Conference on Machine Learning*, pages 1306–1316. PMLR, 2020.
- [6] Simon L Cotter, Gareth O Roberts, Andrew M Stuart, and David White. MCMC methods for functions: modifying old algorithms to make them faster. *Statistical Science*, 28(3):424–446, 2013.
- [7] Lehel Csató and Manfred Opper. Sparse on-line Gaussian processes. *Neural Computation*, 14(3):641–668, 2002.
- [8] Kurt Cutajar, Edwin V Bonilla, Pietro Michiardi, and Maurizio Filippone. Random feature expansions for deep Gaussian processes. In *International Conference on Machine Learning*, pages 884–893. PMLR, 2017.
- [9] Zhenwen Dai, Andreas Damianou, Javier González, and Neil Lawrence. Variational auto-encoded deep Gaussian processes. In *Proceedings of the Fourth International Conference on Learning Representations*, 2016.
- [10] Andreas Damianou and Neil D. Lawrence. Deep Gaussian processes. In *Proceedings of the Sixteenth International Conference on Artificial Intelligence and Statistics*, volume 31 of *Proceedings of Machine Learning Research*, pages 207–215. PMLR, 2013.
- [11] Andreas Damianou, Michalis Titsias, and Neil Lawrence. Variational Gaussian process dynamical systems. *Advances in neural information processing systems*, 24, 2011.
- [12] Daniel Augusto de Souza, Alexander Nikitin, ST John, Magnus Ross, Mauricio A Álvarez, Marc Deisenroth, João Paulo Gomes, Diego Mesquita, and César Lincoln Mattos. Thin and deep Gaussian processes. *Advances in Neural Information Processing Systems*, 36:13138–13148, 2023.
- [13] Arthur P Dempster, Nan M Laird, and Donald B Rubin. Maximum likelihood from incomplete data via the EM algorithm. *Journal of the Royal Statistical Society: Series B (Methodological)*, 39(1):1–22, 1977.
- [14] Matthew Dunlop, Mark Girolami, Andrew Stuart, and Aretha Teckentrup. How deep are deep Gaussian processes? *Journal of Machine Learning Research*, 19:1–46, 2018.
- [15] David Duvenaud, Oren Rippel, Ryan Adams, and Zoubin Ghahramani. Avoiding pathologies in very deep networks. In *Proceedings of the Seventeenth International Conference on Artificial Intelligence and Statistics*, volume 33 of *Proceedings of Machine Learning Research*, pages 202–210. PMLR, 22–25 Apr 2014.
- [16] Gianluca Finocchio and Johannes Schmidt-Hieber. Posterior contraction for deep Gaussian process priors. *Journal of Machine Learning Research*, 24(66):1–49, 2023.
- [17] Helmut Harbrecht, Michael Peters, and Reinhold Schneider. On the low-rank approximation by the pivoted Cholesky decomposition. *Applied Numerical Mathematics*, 62(4):428–440, 2012.
- [18] Helmut Harbrecht, Michael Peters, and Markus Siebenmorgen. Efficient approximation of random fields for numerical applications. *Numerical Linear Algebra with Applications*, 22(4):596–617, 2015.
- [19] James Hensman and Neil D Lawrence. Nested variational compression in deep Gaussian processes. *arXiv preprint arXiv:1412.1370*, 2014.
- [20] Tim Johnston, Francesca Romana Crucinio, O Deniz Akyildiz, Sotirios Sabanis, Mark Girolami, et al. Interacting particle Langevin algorithm for maximum marginal likelihood estimation. *ESAIM: Probability and Statistics*, forthcoming, 2025.

- [21] Daniel Kressner, Jonas Latz, Stefano Massei, and Elisabeth Ullmann. Certified and fast computations with shallow covariance kernels. *Foundations of Data Science*, 2(4):487–512, 2020.
- [22] Juan Kuntz, Jen Ning Lim, and Adam M. Johansen. Particle algorithms for maximum likelihood training of latent variable models. In *Proceedings of The 26th International Conference on Artificial Intelligence and Statistics*, volume 206 of *Proceedings of Machine Learning Research*, pages 5134–5180. PMLR, 2023.
- [23] Jonas Latz, Aretha L Teckentrup, and Simon Urbainczyk. Deep Gaussian process priors for Bayesian image reconstruction. *Inverse Problems*, accepted, 2025.
- [24] Karla Monterrubio-Gómez, Lassi Roininen, Sara Wade, Theodoros Damoulas, and Mark Girolami. Posterior inference for sparse hierarchical non-stationary models. *Computational Statistics & Data Analysis*, 148:106954, 2020.
- [25] Shu Kay Ng, Thriyambakam Krishnan, and Geoffrey J. McLachlan. The EM Algorithm. *James E Gentle, Wolfgang K Härdle, Yuichi Mori (eds.). Handbook of Computational Statistics: Concepts and Methods*, pages 139–172, 2012.
- [26] Conor Osborne and Aretha L. Teckentrup. Convergence rates of non-stationary and deep Gaussian process regression. *Foundations of Data Science*, 2025.
- [27] Christopher Joseph Paciorek. *Nonstationary Gaussian processes for regression and spatial modelling*. PhD thesis, Carnegie Mellon University, 2003.
- [28] Omiros Papaspiliopoulos, Gareth O Roberts, and Martin Sködl. A general framework for the parametrization of hierarchical models. *Statistical Science*, pages 59–73, 2007.
- [29] Yuan (Alan) Qi, Ahmed H. Abdel-Gawad, and Thomas P. Minka. Sparse-posterior Gaussian processes for general likelihoods. *CoRR*, abs/1203.3507, 2012.
- [30] Joaquin Quiñero-Candela and Carl Edward Rasmussen. A unifying view of sparse approximate Gaussian process regression. *Journal of Machine Learning Research*, 6(65):1939–1959, 2005.
- [31] Lassi Roininen, Mark Girolami, Sari Lasanen, and Markku Markkanen. Hyperpriors for Matérn fields with applications in Bayesian inversion. *Inverse Problems and Imaging*, 13(1):1–29, 2019.
- [32] Simone Rossi, Markus Heinonen, Edwin Bonilla, Zheyang Shen, and Maurizio Filippone. Sparse Gaussian processes revisited: Bayesian approaches to inducing-variable approximations. In *International Conference on Artificial Intelligence and Statistics*, pages 1837–1845. PMLR, 2021.
- [33] Annie Sauer, Andrew Cooper, and Robert B Gramacy. Non-stationary Gaussian process surrogates. *arXiv preprint arXiv:2305.19242*, 2023.
- [34] Annie Sauer, Robert B. Gramacy, and David Higdon. Active learning for deep Gaussian process surrogates. *Technometrics*, 65(1):4–18, 2023.
- [35] Alex J. Smola and Peter Bartlett. Sparse greedy Gaussian process regression. In *Proceedings of the 14th International Conference on Neural Information Processing Systems, NIPS’00*, page 598–604. MIT Press, 2000.
- [36] Rolf Sundberg. Maximum likelihood theory for incomplete data from an exponential family. *Scandinavian Journal of Statistics*, pages 49–58, 1974.
- [37] Michalis K Titsias. Variational model selection for sparse Gaussian process regression. *Report, University of Manchester, UK*, 2009.
- [38] Michalis K Titsias. Variational learning of inducing variables in sparse Gaussian processes. In *Proceedings of the Twelfth International Conference on Artificial Intelligence and Statistics*, volume 5 of *Proceedings of Machine Learning Research*, pages 567–574. PMLR, 16–18 Apr 2009.

- [39] Greg C G Wei and Martin A Tanner. A Monte Carlo implementation of the EM algorithm and the poor man's data augmentation algorithms. *Journal of the American statistical Association*, 85(411):699–704, 1990.
- [40] Christopher K I Williams and Carl Edward Rasmussen. *Gaussian processes for machine learning*, volume 2. MIT Press Cambridge, MA, 2006.
- [41] Christopher K I Williams and Matthias Seeger. Using the Nyström method to speed up kernel machines. In *Proceedings of the 14th International Conference on Neural Information Processing Systems, NIPS'00*, page 661–667. MIT Press, 2000.
- [42] Han Xiao, Kashif Rasul, and Roland Vollgraf. Fashion-MNIST: A novel image dataset for benchmarking machine learning algorithms. *arXiv preprint arXiv:1708.07747*, 2017.
- [43] Yaming Yu and Xiao-Li Meng. To center or not to center: That is not the question — An ancillarity–sufficiency interweaving strategy (ASIS) for boosting MCMC efficiency. *Journal of Computational and Graphical Statistics*, 20(3):531–570, 2011.